JOURNAL OF MATERIALS SCIENCE 27 (1992)1311 - 1316

Hot ductility of simulated stainless-steel weld metals

Z. SUN
Department of Mechanical Engineering, Lappeenranta University of Technology, SF-53851 Lappeenranta, Finland

H. Y. HAN
Department of Welding, Central Iron and Steel Research Institute, 100081 Beijing, People's Republic of China

Simulation of stainless-steel weld metals was performed using a Gleeble-1500 thermomechanical simulator. Two classes of materials were investigated, including both fully austenitic and austenitic–ferritic stainless steels. The niobium content varied within each class. The simulation comprised heating to melting point, melting for a short time, and cooling to a number of temperatures, at which point the samples were fractured under a tensile load. The hot ductility, in terms of reduction of area, was measured. Metallographic examinations were performed using both optical and electron microscopy. The hot ductilities of the austenitic–ferritic weld metals investigated were superior to those of fully austenitic weld metals of corresponding niobium content. The beneficial effects of ferrite were found to decrease with increasing niobium content. The effect of niobium on hot ductility was detrimental, i.e. an increase in niobium content resulted in a decrease in hot ductility which was attributed to the formation of $(FeCrNi)_2Nb$-γ, a low melting eutectic, along the austenitic grain boundaries. The criterion of hot ductility by simulation of the weld metals was also found to be reliable for evaluating susceptibility to solidification cracking.

1. Introduction

Weld thermal simulation has played an important role in the understanding of welding metallurgy during the last few decades. The technique has been applied extensively to simulate the heat-affected zone, either to study the microstructures and mechanical properties in different regions within the heat-affected zone, or to evaluate the liquation cracking tendency [1–9]. Most of the work on weld thermal simulation has been carried out in a peak temperature range below the melting point of the material. However, simulations of the weld metal are few due to difficulties in reproducing the heating and cooling process. Sopher *et al.* [10] and Cordea *et al.* [11] have evaluated the hot cracking tendency of weld metals by using an induction heating simulator. Weld simulation up to the molten state has also been carried out by Kussmaul *et al.* [12] to investigate the influence of multipass effects on the solidification structures of the weld metals. In the present work, simulation of stainless steel weld metals was performed using a resistance heating Gleeble-1500 machine to study their hot ductility and thus their susceptibility to solidification cracking.

Kang *et al.* [13] reported that 00Cr25Ni20Nb steel offers excellent corrosion resistance in a mixed acid (mainly nitric) environment. Its corrosion resistance was not reduced after 2 h sensitization at 600–850 °C. A weldability study has shown that hot cracking is a problem in which niobium plays an important role (H.Y.H., unpublished results). The contradiction of the effect of niobium on the corrosion and weldability properties makes it necessary to evaluate its influence. Although an effect of niobium on hot-cracking sensitivity in highly alloyed steels has been described [14], a study of its effect on this specific alloy is still required in order to make the steel more applicable. Many studies have shown that a certain amount of ferrite in austenitic stainless steel weld metal reduces the risk of hot cracking [15–17], thus the effect of ferrite was also investigated.

2. Experimental procedure

2.1. Materials

The steels used in this study were melted by the vacuum induction process. The ingots were forged and hot rolled into 14-mm thick plate, after which they were solution heat-treated at 1080 °C for 30 min, followed by water quenching. Chemical analyses of the steels are given in Table I. The steels were divided into two classes: fully austenitic and austenitic–ferritic, depending on the nickel content. The niobium content was varied from 0–1.6% within each class. To isolate the effect of niobium, the carbon, sulphur and phosphorous contents were kept low.

2.2. Experimental procedure

Simulation of weld metals was conducted using a

0022–2461

TABLE I Chemical compositions of the test alloys (wt %)

No.	C	Si	Mn	S	P	Cr	Ni	Nb
1	0.003	0.25	1.22	0.004	0.010	24.95	19.78	< 0.10
2	0.004	0.24	1.25	0.004	0.007	25.05	19.78	0.38
3	0.004	0.25	1.24	0.004	0.004	25.03	19.75	0.75
4	0.003	0.24	1.22	0.004	0.004	25.08	19.98	1.12
5	0.003	0.24	1.24	0.004	0.004	24.93	19.56	1.66
6	0.003	0.25	1.20	0.004	0.009	25.00	17.54	< 0.10
7	0.002	0.24	1.22	0.004	0.006	24.98	17.51	0.37
8	0.003	0.24	1.24	0.004	0.004	25.13	17.54	0.74
9	0.002	0.23	1.25	0.004	0.004	24.95	17.41	1.10
10	0.002	0.24	1.20	0.004	0.004	25.05	17.16	1.60

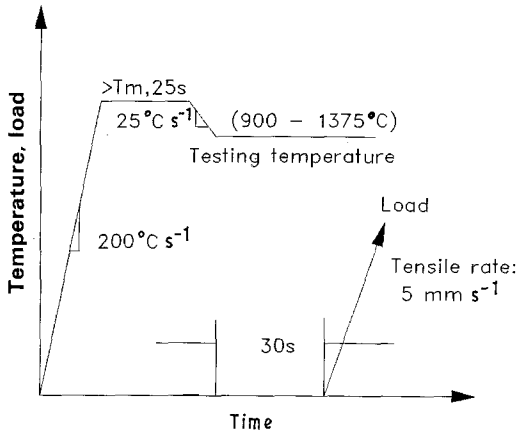

Figure 1 Schematic diagram of the variables used in simulation tests of stainless-steel weld metals.

Gleeble-1500 thermomechanical simulator. The test specimens, 10 mm in diameter and 125 mm long, were machined in the rolling direction. A 20-mm-long section in the centre of the samples was heated to the molten state in order to simulate the conditions of heating and solidification of the weld metal, followed by cooling to a certain temperature, at which point the samples were fractured under a tensile load. A quartz tube, with a small longitudinal slot for accommodating a thermocouple, was used to prevent molten metal from flowing and changing shape. The temperature was measured with a ϕ0.25-mm PtRh–Pt thermocouple welded onto the surface of the sample. To avoid oxidation, the test was performed in a sealed chamber filled with pure argon gas. A schematic diagram of the variables used in the test is shown in Fig. 1. The parameters were programmed and controlled using an IBM personal computer. Subsequent to the tensile test, the reduction of area was measured using a micrometer to specify the hot ductility of the simulated weld metals. Metallographic work was performed on the simulated samples. An electrolytic etch using 10% oxalic acid was made to reveal the microstructures of the simulated weld metals. Both optical and electron microscopy were used for microstructural characterization and fracture surface observation. Transmission electron microscopy (TEM) and physical phase analysis were also applied to identify the low melting phase. More details of the experimental procedure can be found elsewhere [18].

3. Results

3.1. Hot ductility of austenitic weld metals

The hot ductility of the simulated austenitic weld metals as a function of temperature is shown in Fig. 2. The tendency for all the materials illustrated was that hot ductility increased with decreasing testing temperature, from zero to a peak ductility, and then decreased slowly. However, the rate at which hot ductility was regained and the peak value of the hot ductility were different from each other. Hot ductility depends on both factors, but the regain rate was more important, as hot ductility is a property in a high temperature range rather than a single value at one temperature. Scanning electron microscope (SEM) observations showed that the regain rate of hot ductility from the high to the lower temperature resulted in a change in fracture surface from brittle to ductile, as shown in Fig. 3. The fracture surface of the hot ductility sample tested at 1300 °C exhibited typical brittle intergranular fracture along the, natural solidification grain boundaries, whereas the surface of the sample tested at 1200 °C showed many deep dimples, indicating that the hot ductility had been improved significantly. The decrease after the peak ductility value led to another trough (not shown in Fig. 2). This region is referred to as the ductility-dip temperature range [19]. This phenomenon has been observed in simulated stainless steel weld metals (Z.S., unpublished data)—its study is beyond the scope of this investigation.

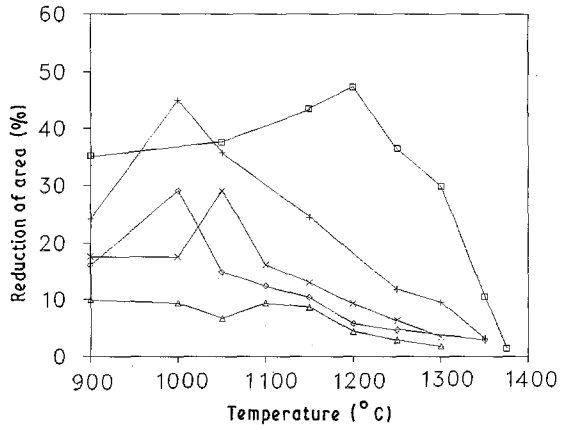

Figure 2 Hot ductility curves of the simulated austenitic stainless-steel weld metals showing the influence of niobium. Steel no. □, 1; +, 2; ◇, 3; △, 4; ×, 5.

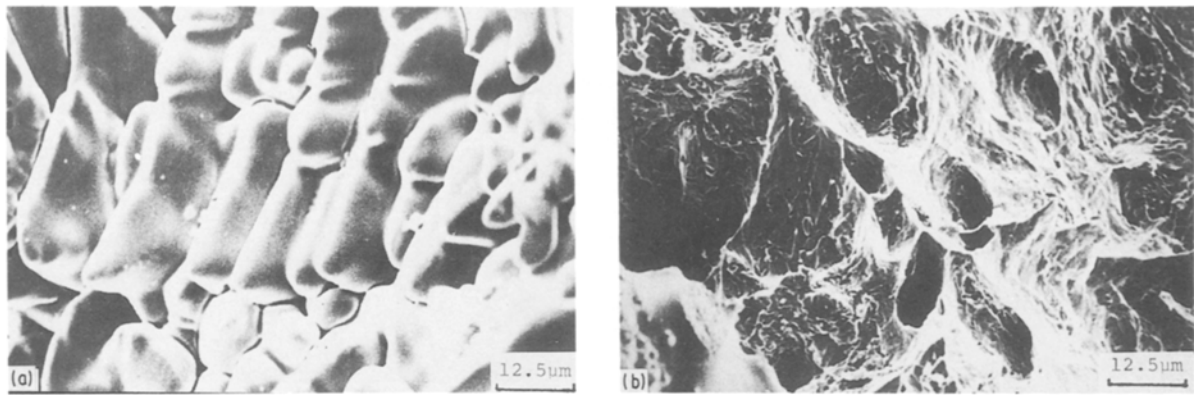

Figure 3 Typical fracture surfaces of the simulated austenitic stainless-steel weld metals observed in SEM. Steel 1, tested at (a) 1300 and (b) 1200 °C.

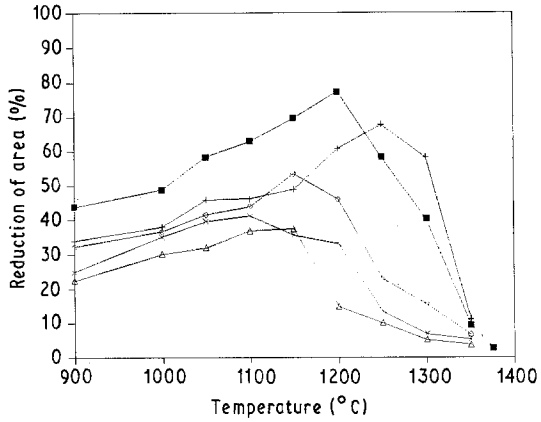

Figure 4 Hot ductility curves of the simulated austenitic-ferritic stainless-steel weld metals showing the influence of niobium. Steel no. ■, 6; +, 7; ◇, 8; △, 9; ×, 10.

From the curves we can see that hot ductility decreases with increasing niobium content to a critical value, and then increases. This is the effect of niobium on the hot ductility of austenitic weld metals, which is discussed later.

3.2. Hot ductility of austenitic–ferritic weld metals

The hot ductility of the simulated austenitic–ferritic weld metals as a function of testing temperature is shown in Fig. 4. There was about 5% ferrite in all the simulated austenitic–ferritic weld metals [18]. The same tendency is found from the curves, showing that the hot ductility increased with a decrease in testing temperature and then decreased beyond the peak value. The effect of niobium on the hot ductility of austenitic–ferritic weld metals is similar to that of austenitic weld metals.

4. Discussion

4.1. Effect of niobium

The effect of niobium on the hot ductility of both fully austenitic and austenitic–ferritic stainless-steel weld metals is shown in Figs 2 and 4, respectively. The sample without niobium (Steel 1) exhibited good hot ductility due to the very clean austenitic grain boundaries. For low niobium contents, the hot ductility of fully austenitic weld metals decreased with an increase

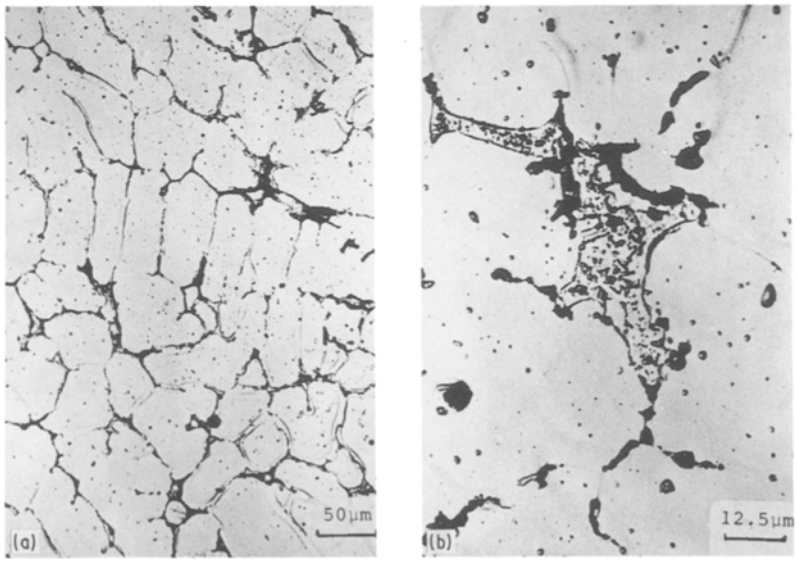

Figure 5 (a, b) Typical morphology of low-melting eutectic Steel 5 tested at 1200 °C at different magnifications.

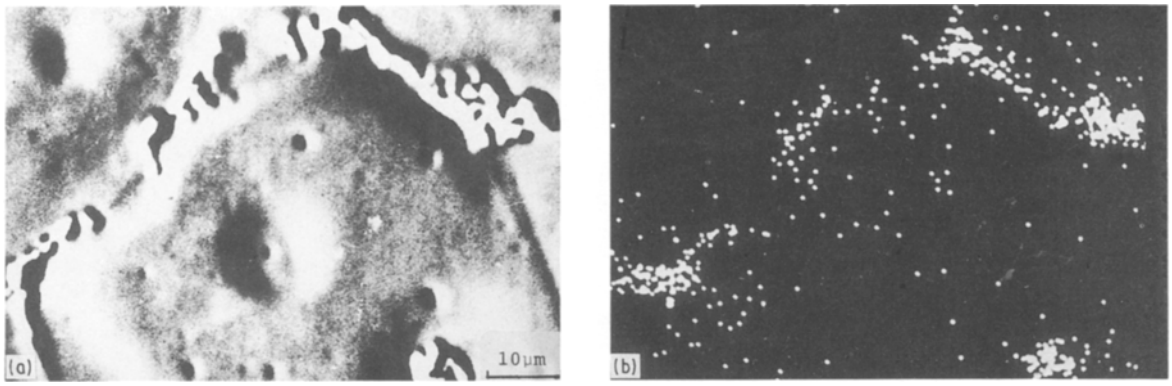

Figure 6 Electron microprobe analysis results showing the distribution of niobium. (a) Electron scanning image, (b) X-ray maps for Nb correspond to the field of view in (a).

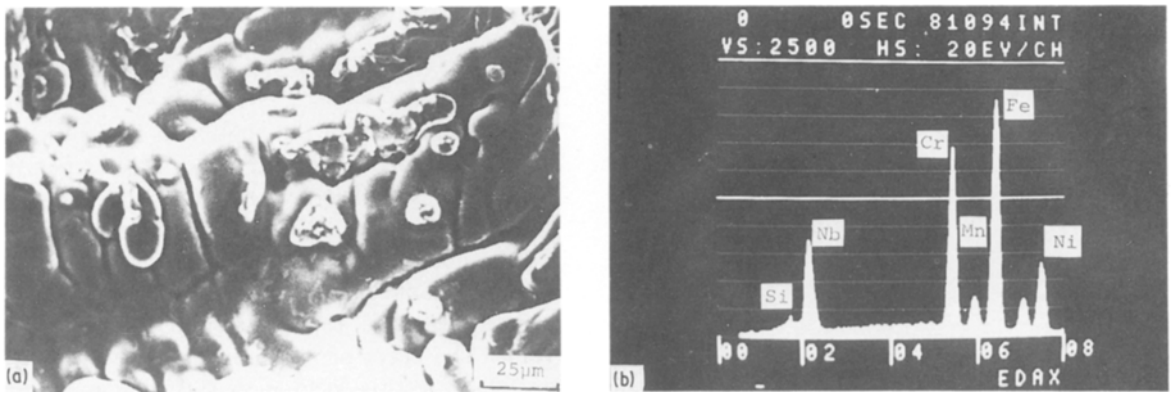

Figure 7 SEM micrograph showing the Nb-rich low-melting eutectic along the austenitic grain boundaries. (a) Steel 5 tested at 1200 °C; (b) EDX results.

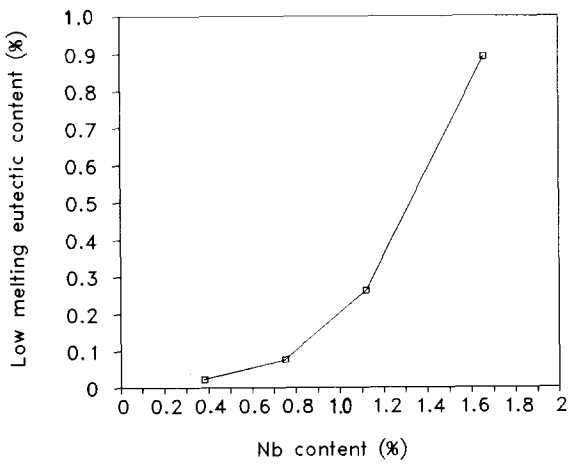

Figure 8 Weight fraction of eutectic against niobium content for the simulated austenitic stainless-steel weld metals.

in niobium content up to a critical level (1.1%). Microscopic examination of the simulated samples showed that a low-melting eutectic segregated along the austenitic grain boundaries, especially at the triple points (Fig. 5). Electron microprobe analysis (EMPA) revealed the presence of an Nb-rich low-melting eutectic in the Nb-bearing simulated weld metal (Fig. 6). SEM observations (Fig. 7) and quantitative phase analysis (Fig. 8) of the simulated fully austenitic samples indicated that an increase in niobium content resulted in an increase in the low-melting phase. Further studies by TEM and phase analysis identified that the low-melting eutectic was $(FeCrNi)_2Nb$-γ [18]. The eutectic temperature of $(FeCrNi)_2Nb$-γ is in the range 1275–1270 °C [20], which is significantly lower than the melting point of the matrix. The Nb-rich, low-melting eutectic was responsible for the decrease in hot ductility due to its low strength. The same tendency can be found in austenitic–ferritic weld metals.

Above a critical niobium content, however, a beneficial effect of increasing the amount of niobium occurs. This phenomenon may be related to two effects. One is the healing effect of low-melting eutectic [14]. If low-melting eutectic is present in sufficient quantity, it can fill the cracks as they are formed until solidification is complete, thus improving the hot ductility. The analysis of this study has shown that the amount of low-melting eutectic increased with increasing niobium content, thus the healing effect may explain the findings. The other reason is the advantageous effect of a small amount of ferrite. Steel 5 has 1.66% Nb, which is a ferrite-forming element: its position in the Schaeffler diagram shows that there is about 1–2% ferrite in the weld metal, which was confirmed in the metallographic observations [18]. Steel 10 also has the highest ferrite content among the steels.

4.2. Effect of ferrite

Fig. 9 shows the comparison of hot ductilities between austenitic and austenitic-ferritic weld metals with

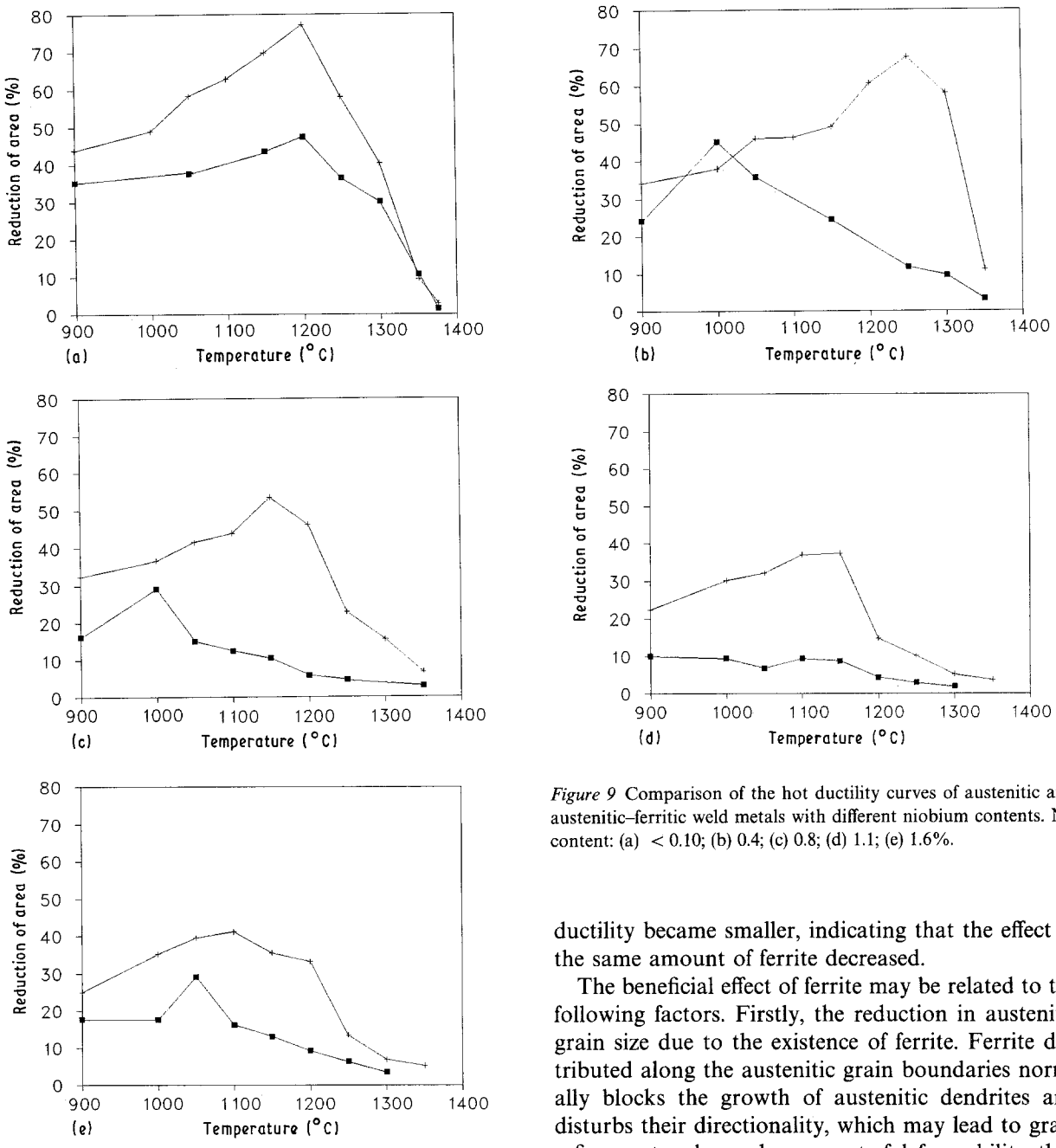

Figure 9 Comparison of the hot ductility curves of austenitic and austenitic–ferritic weld metals with different niobium contents. Nb content: (a) < 0.10; (b) 0.4; (c) 0.8; (d) 1.1; (e) 1.6%.

different niobium contents. The hot ductilities of all the austenitic–ferritic weld metals are superior to those of corresponding austenitic weld metals for all the niobium contents investigated here. It can be seen that the influence of ferrite decreases with an increase in niobium content. When no niobium is present (Fig. 9a) the temperatures corresponding to the peak values of reduction of area are almost the same for both austenitic and austenitic–ferritic weld metals, but the peak temperatures for austenitic weld metals were reduced when the niobium contents were 0.4 and 0.8%. This suggests that the beneficial effect of ferrite is significant in this niobium content range, i.e., the rate of regain of hot ductility of austenitic–ferritic weld metals is much faster, and their brittleness temperature ranges are much narrower, than those of fully austenitic weld metals. However, when the niobium content increased to 1.1 to 1.6%, the difference between the temperatures corresponding to the peak ductility became smaller, indicating that the effect of the same amount of ferrite decreased.

The beneficial effect of ferrite may be related to the following factors. Firstly, the reduction in austenitic grain size due to the existence of ferrite. Ferrite distributed along the austenitic grain boundaries normally blocks the growth of austenitic dendrites and disturbs their directionality, which may lead to grain refinement and an enhancement of deformability, thus improving the hot ductility. This has been verified in an optical examination of the simulated samples [18]. Secondly, ferrite has a greater solubility than austenite for certain harmful elements and impurities such as Nb, S, P and Si. Segregation of these elements at the grain boundaries, and consequently the extent of liquid film formation, is reduced during solidification thus increasing the hot ductility. For example, the analysis of steel 10 using EMPA showed that there was 0.84% Nb in the austenitic matrix, and 2.19% Nb in the ferrite. In addition, a small amount of Nb-rich eutectic was found during the SEM observation of steels 8, 9 and 10, whereas no Nb-rich eutectic was found in steels 6 and 7 due to the small Nb content, hence their hot ductilities are excellent. Finally, the smaller coefficient of thermal expansion of ferrite can also contribute to improving the hot ductility.

4.3. Application of the simulation test

The solidification crack susceptibility of weld metals

using hot ductility data obtained from this simulation test has been evaluated elsewhere [21, 22]. Solidification cracking in weld metals often occurs during the final stage of solidification, when the strains resulting from thermal and solidification shrinkage exceed the ductility of the partially solidified metal. Thus it is theoretically rational to examine solidification-crack susceptibility using hot ductility as a criterion. The better the hot ductility, the smaller the solidification crack susceptibility. In fact, a comparative study using both the stimulation test and the Transvarestraint test established a fairly good correlation and indicated that the results obtained from the simulation test are reliable [21, 22].

5. Conclusions

A hot ductility study of simulated stainless-steel weld metals has been performed using a Gleeble-1500 simulator. The following conclusions can be drawn from this investigation.

1. The hot ductility of simulated stainless steel weld metals decreases on increasing the niobium content to a critical value, beyond which an improvement is observed. The detrimental effect of niobium at low concentrations is attributed to the formation of Nb-rich low-melting eutectic $(FeCrNi)_2Nb$-γ along the austenitic grain boundaries.

2. All the hot ductilities of the austenitic–ferritic weld metals are superior to those of fully austenitic weld metals of corresponding niobium content. The beneficial effects of ferrite are due to the grain refinement, greater solubility of certain harmful elements or impurities, and the smaller coefficient of thermal expansion. The influence of ferrite decreases with an increase in niobium content.

3. The critical value for the effect of niobium is related to the synergistic effects of the healing function of sufficient low-melting eutectic, and the beneficial effect of a small amount of ferrite.

4. The hot ductility criterion can be used for estimating the solidification crack susceptibility of weld metals.

Acknowledgements

The authors would like to thank the staff of the simulation group in the Welding Department of CISRI for their assistance in the simulation tests. They also wish to thank Dr J. C. Ion for revising the English of the manuscript.

References

1. E. F. NIPPES and W. F. SAVAGE, *Welding J.* **28** (1949) 534.
2. E. F. NIPPES, W. F. SAVAGE, B. J. BASTIAN, H. F. MASON and R. M. CURRAN, *ibid.* **34** (1955) 183.
3. C. S. WILLIAMS, *ibid.* **42** (1963) 1.
4. W. A. OWCZARSKI, D. S. DUVALL and C. P. SULLIVAN, *ibid.* **45** (1966) 145.
5. K. C. WU and R. E. HERFERT, *ibid.* **46** (1967) 32.
6. W. DAHL, C. DUREN and H. MUSCH, Document II-660-73 (International Institute of Welding, 1973).
7. W. LIN, W. A. BAESLACK III and J. C. LIPPOLD, in Proceedings of the 2nd International Conference on Trends in Welding Research Gatlinburg, Tennessee, May 1989, edited by S. A. David and J. M. Vitek (ASM International, Ohio, 1990) p. 609.
8. J. M. VITEK and S. A. DAVID, *Metall. Trans. A.* **21A** (1990) 2021.
9. S. A. DAVID, J. A. HORTON, G. M. GOODWIN, D. H. PHILLIPS and R. W. REED, *Welding J.* **69** (1990) 133.
10. R. P. SOPHER, A. J. JACOBES and P. J. RIEPPEL, *ibid.* **34** (1955) 544.
11. J. N. CORDEA, P. A. KAMMER and D. C. MARTIN, *ibid.* **43** (1964) 481.
12. K. KUSSMAUL, R. SCHWAB and J. N. AOH, in Proceedings of the 1st International Conference on Trends in Welding Research, Gatlinburg, Tennessee, May 1986, edited by S. A. David (ASM International, Ohio, 1986) p. 127.
13. X. F. KANG and D. K. ZHANG, in "Special Issue in Stainless Steels" (Beijing, 1981) p. 95.
14. R. CASTRO and J. J. De CADENET, in "Welding Metallurgy of Stainless and Heat Resisting Steels" (Cambridge University Press, London, 1974) p. 142.
15. J. C. BORLAND and R. D. YOUNGER, *Brit. Weld. J.* **7** (1960) 22.
16. F. C. HULL, *Welding J.* **46** (1967) 399.
17. Y. ARATA, F. MATSUDA and S. KATAYAMA, *Trans. Japanese Welding Research Institute* **5** (1976) 35.
18. Z. SUN, M. Eng. thesis, Central Iron and Steel Research Institute, Beijing, China, 1987.
19. B. HEMSWORTH, T. BONISZEWSKI and N. F. EATON, *Metal Constr. Brit. Weld. J.* **1** (1969) 5.
20. F. MATSUDA, H. NAKAGAWA, S. KATAYAMA and Y. ARATA, *Trans. JWRI* **11** (1982) 79.
21. Z. SUN and H. Y. HAN, Document IX-1604-90 (International Institute of Welding, 1990).
22. Z. SUN and H. Y. HAN, *J. Mater. Sci. Lett.* **10** (1991) 747.

Received 17 December 1990
and accepted 13 May 1991